Hydrogel droplet microarrays with trapped antibody-functionalized beads for multiplexed protein analysis

Huiyan Li,[ab] Rym Feriel Leulmi[ab] and David Juncker*[abc]

Received 11th August 2010, Accepted 4th November 2010
DOI: 10.1039/c0lc00291g

Antibody microarrays are a powerful tool for rapid, multiplexed profiling of proteins. 3D microarray substrates have been developed to improve binding capacity, assay sensitivity, and mass transport, however, they often rely on photopolymers which are difficult to manufacture and have a small pore size that limits mass transport and demands long incubation time. Here, we present a novel 3D antibody microarray format based on the entrapment of antibody-coated microbeads within alginate droplets that were spotted onto a glass slide using an inkjet. Owing to the low concentration of alginate used, the gels were highly porous to proteins, and together with the 3D architecture helped enhance mass transport during the assays. The spotting parameters were optimized for the attachment of the alginate to the substrate. Beads with 0.2 μm, 0.5 μm and 1 μm diameter were tested and 1 μm beads were selected based on their superior retention within the hydrogel. The beads were found to be distributed within the entire volume of the gel droplet using confocal microscopy. The assay time and the concentration of beads in the gels were investigated for maximal binding signal using one-step immunoassays. As a proof of concept, six proteins including cytokines (TNFα, IL-8 and MIP/CCL4), breast cancer biomarkers (CEA and HER2) and one cancer-related protein (ENG) were profiled in multiplex using sandwich assays down to pg mL^{-1} concentrations with 1 h incubation without agitation in both buffer solutions and 10% serum. These results illustrate the potential of beads-in-gel microarrays for highly sensitive and multiplexed protein analysis.

Introduction

Multiplexed profiling of protein disease biomarkers for early diagnostics requires a highly sensitive and reliable technology to accurately quantify multiple proteins. Both beads[1–3] and antibody microarrays[4–7] have recently emerged as promising technologies for multiplexed profiling and quantification of proteins. For microarrays on solid supports, glass slides with different surface chemistries including epoxy, or amino-silane, poly-L-lysine, and streptavidin have been used and characterized.[8–10] Overnight sample incubation is commonly required to obtain pg mL^{-1} detection limits, and many efforts are underway to shorten the assay time and improve sensitivity such as the development of microfluidic systems and the addressable nanolitre well plates for biological assays.[11,12] Hydrogels have been coated as thin layers on glass slides and used for immunoassays because the gel itself could serve as support to bind proteins and thus help increase the binding signals compared to 2D substrates. Proteins have been spotted and immobilized *via* cross-linking onto poly(ethyl glycol),[13] poly(vinyl alcohol),[13–15] polyurethane,[16] carboxymethylated dextran[17] and polyacrylamide[18] and agarose coated slides.[19] In each case, the hydrogel led to higher protein loading capacity, higher fluorescent signals, and better spot morphology compared to a 2D surface. Some of the drawbacks and limitations of hydrogels are that linkage of proteins to the gel remains laborious, and that proteins diffuse within the gels after spotting enlarging each spot and limiting spot density of the array, while at the same time the cross-linked gels hinder mass transport and the diffusion of analytes to the capture antibodies, thus requiring longer incubation time and reducing sensitivity. To overcome some of these limitations, gel droplet biochips that rely on spotting the hydrogels as droplets were developed using both polyacrylamide and polymethacrylamide gels.[20–22] Diffusion of proteins following spotting was thus constrained, and the assay reproducibility was better than that on equivalent thin layer slides. Although the droplet shape is more readily accessible to analytes from solution, the small pore size of cross-linked gels still limited mass transport.

An alternative approach to increase binding surface of slides was proposed by Stevens and colleagues who spotted microbeads coated with capture probes onto hydrogel slides.[23] However, because the beads were spotted on a planar surface, long incubation times of 8 h were required to reach reaction equilibrium between IgG molecules. Another group mixed melamine particles coated with a fluorescent IgG suspended with different hydrogels to explore whether it could help increase the fluorescent signal intensities, and polyvinyl alcohol was identified as a promising material.[14] However, a pin spotter was used which raised the question of spot morphology and bead distribution, but none of which were characterized, and the beads appeared to be leaching out of many gel constructs. Moreover, no immunoassays were performed, and the potential for multiplexing could thus not be assessed. Baba and colleagues recently presented data on hydrogels as a scaffold material for trapping antibody coated

[a]*Biomedical Engineering Department, McGill University, Montréal, QC, H3A 1A4, Canada. E-mail: david.juncker@mcgill.ca*
[b]*McGill University and Genome Quebec Innovation Centre, McGill University, Montréal, QC, H3A 1A4, Canada*
[c]*Department of Neurology and Neurosurgery, McGill University, Montréal, QC, H3A 1A4, Canada*

beads within the gel in a 3D volume.[24] Hydrogel posts were photopatterned within a microchannel and each post contained a mixture of antibody coated beads. This approach helped improve the diffusive flux of antigens to the antibody coated beads because of the distribution of the beads in 3D, and because the flow contributed to replenish the antigens around the posts. However, the multiplexing ability of this platform is limited because different beads coated with different capture antibodies are mixed within one post, and thus a different fluorescent dye is needed for each antibody; only 4–5 colors may be resolved using a conventional fluorescent microscope or a microarray scanner. Recently, another approach for trapping beads in gels was proposed based on a layer-by-layer assembly achieved by repeated dipping of a slide into different agarose solutions with beads, followed by gelation at each step. Slides with multiple layers each containing one type of beads were thus formed.[25] The advantage of this technique is simplicity, and high sensitivity of immunoassays which extended into the pM range, albeit overnight incubation was needed to allow for reagents to diffuse through the thick agarose gels. Three layers were demonstrated, and the multiplexing ability will likely be limited by the need to image across the bottom layers to capture the fluorescence of the beads in the top layers which is problematic due to scattering by the beads.

In this manuscript, we present a novel antibody microarray platform that we call beads-in-gel droplet microarray (BiGDM) using alginate gels containing microbeads to form droplets on a glass slide. Microbeads were coated with capture antibodies by adsorption and mixed with alginate solutions. Droplets of the solutions were arrayed onto glass slides using an inkjet spotter. Next, the alginate droplets containing the beads were solidified by incubating the entire slide in a calcium solution. Bead size and concentration were optimized using fluorescent beads and one-step immunoassays. Finally, BiGDM was used for multiplexed sandwich immunoassays for the detection of 6 proteins including cytokines and breast cancer biomarkers in buffer solutions and 10% serum. We obtained pg mL^{-1} detection limits with 1 h sample incubation without agitation.

Experimental

Materials

Polystyrene microspheres with diameters of 0.2 μm, 0.5 μm, and 1 μm were purchased from Polysciences, Inc. Low viscosity alginic acid sodium salt, boric acid, glycerol, sodium azide, Tris base, calcium chloride, and Tween 20 were obtained from Sigma-Aldrich. Bovine serum albumin (BSA) was purchased from Jackson ImmunoResearch Laboratories, Inc. Alexa Fluor 532 goat anti-mouse IgG (H + L) and Alexa Fluor 647 chicken anti-goat IgG (H + L) were purchased from Invitrogen. Antibody and antigen pairs used in this study include Interleukin 8 (IL-8) from Invitrogen, Carcinoembryonic Antigen (CEA) from US Biological, Endoglin (ENG), Human Epidermal growth factor Receptor 2 (HER2), macrophage inflammatory protein 1β (CCL4/MIP-1β), and tumor necrosis factor-α (TNFα) from R&D Systems. Normal human female serum from a single donor was purchased from Golden West Biologicals. Aminosilane coated slides were purchased from Schott North America.

Coating beads with antibodies

0.1 M borate buffer at pH 8.5 was prepared. 0.1 mL polystyrene beads were washed twice in 0.2 mL borate buffer in an Eppendorf tube by centrifuging at 7400 rpm for 4.5 minutes followed by removal of the supernatant. After re-suspending the beads pellet in 0.2 mL borate buffer, 40 μL of 2 mg mL^{-1} antibodies were added. The solution was gently mixed by pipetting and incubated overnight at 4 °C. Then the beads solution was centrifuged and the supernatant was removed. After blocking with 1% BSA for 1 h, the beads were washed once, and re-suspended in 0.2 mL storage PBS buffer containing 0.88% NaCl, 1% BSA, 5% glycerol, and 0.1% NaN_3.

Microarray fabrication

The BiGDM was fabricated by spotting alginate solution mixed with beads onto aminosilane coated glass slides, followed by incubation with 0.2 M $CaCl_2$ resulting in hydrogel gelation. The spotting solution was prepared using alginate dissolved in DI water with beads in storage buffer and glycerol mixed so as to obtain a final alginate concentration of 0.65%, a bead concentration between 1.9×10^9 particles per mL and 3.04×10^{10} particles per mL depending on the experiments, and 10% glycerol. Spotting was performed using an inkjet spotter (Nanoplotter 2.0, GeSiM). To prevent evaporation during spotting, the sample plate was cooled 3 °C below the room temperature and the relative humidity was set to 80–85%. Each spot contained approximately 2 nL. Spots were separated by 700 or 800 μm center-to-center depending on the experiments. The slide was incubated for 1 h in a chamber saturated with humidity, and dried at room temperature with a humidity of 40% for 10 minutes. A slide module gasket with 16 modules (Grace Bio-Labs, Inc.) was clamped on the slide dividing it into 16 wells for immunoassays. Next, 80 μL of a 0.2 M $CaCl_2$ solution were pipetted into each well to trigger the gelation of alginate and left there for 10 minutes. The slide was rinsed once and could then be used for immunoassays. The first two steps in Fig. 1 show the microarray fabrication process.

Investigation of bead concentration and sample incubation time

Tris buffer at pH 7.5 with 0.05% Tween-20 and 0.01 M $CaCl_2$ was used as the assay buffer. One-step assays using IgG molecules were performed to investigate the effect of bead concentrations on assay sensitivity and dynamic range. Beads were coated with Alexa 532 goat anti-mouse IgG molecules for specific bindings and BSA for the negative controls. Concentrations of the beads at 1.9×10^9 particles per mL, 7.6×10^9 particles per mL, and 3.04×10^{10} particles per mL in alginate solutions were used for comparison. To prevent non-specific binding the slide was incubated in 1% BSA followed by washing twice with assay buffers. Seven dilutions of Alexa 647 chicken anti-goat IgG from 100 μg mL^{-1} to 100 pg mL^{-1} were prepared and applied on slides and incubated for 2 h at room temperature. The slides were then washed 3 times with assay buffer, 5 minutes each time and once with DI water for 5 minutes, by adding 80 μL solutions in each well, and dried before scanning. To investigate the sample incubation time, concentrations of the beads at 3.04×10^{10} particles per mL were used and seven dilutions of chicken

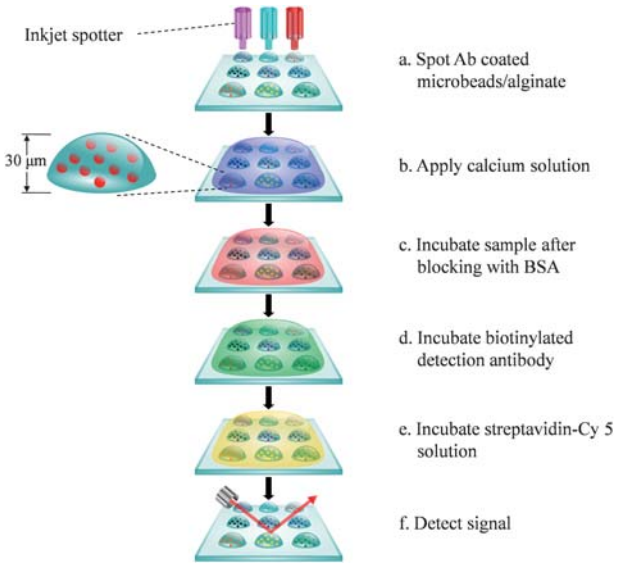

Fig. 1 Fabrication of BiGDM and its use for multiplexed sandwich immunoassays. (a) Alginate solutions were mixed with antibody-coated beads and spotted on a slide using an inkjet spotter. (b) After spotting, the slides were soaked in calcium solution for alginate gelation, thus forming 3D hydrogel structures. This slide was either stored, or used immediately for a sandwich immunoassay. (c) First, the slide was incubated with sample solution, (d) followed by the detection antibody that was labelled with biotin, (e) and then streptavidin–Cy5. (f) Following drying, a fluorescence image of the slide was acquired using a microarray scanner.

anti-goat IgG were applied on slides and incubated for 1 h or 2 h at room temperature.

BiGDM sandwich immunoassays

In our sandwich ELISA assays, 6 breast cancer biomarkers, CEA, ENG, HER2, TNFα, IL-8, and MIP/CCL4 were investigated using bead concentration of 3.04×10^{10} particles per mL for the assays using both spiked buffer or spiked, diluted serum (10% in buffer) as the sample. After blocking with BSA for 1 h and rinsing with assay buffer once for 5 minutes, the slides were incubated for 1 h with the sample solutions containing a mixture of 6 proteins that were spiked into the buffer or the 10% serum solution depending on the experiment. A dilution series was used to establish a binding curve with the protein concentration ranging from 100 to 0.006 ng mL^{-1} for CEA, ENG, and HER2, and from 10 to 0.0006 ng mL^{-1} for TNFα, IL-8, and MIP/CCL4, with a dilution factor of 5, and a control with 0 ng mL^{-1} for all the six proteins. Then the slides were rinsed 3 times with buffer solutions, 5 minutes each time and incubated with a mixture of biotinylated detection antibodies at 1 μg mL^{-1} for 1 h, rinsed using the same procedure as in the previous step and incubated with 1 μg mL^{-1} of streptavidin conjugated to Cy5 dye for 1 h. The final rinsing steps were identical to the protocol used in the one-step assays, and finally the slides were dried.

Scanning and analysis

Slides were scanned using a commercial microarray laser scanner (LS Reloaded™ Tecan, Männedorf, Switzerland). In one-step assays, 532 nm laser was used to evaluate the effects of beads concentrations. For both one-step and sandwich assays, 633 nm laser was used to measure assay signals. The experiments were performed in triplicate, and SigmaPlot software was used to generate binding curves and the sandwich assay detection limit was determined from the negative controls with no antigen incremented by three times the standard deviation.

Results and discussion

Fabrication of BiGDM

The procedure to fabricate alginate-based BiGDM is shown in Fig. 1, steps a and b. Commonly 1–3% of alginate is used to produce hydrogels,[26–28] but the high viscosity of the solutions prevented ink-jetting, and gels with only 0.65% of alginate were therefore used here.

An important challenge to the fabrication of BiGDM was the initial lack of adhesion of the alginate to the glass slide surface. Therefore, aminosilane coated slides with a positively charged surface were used to help immobilize the negatively charged alginate droplets. To further improve the adhesion between the spotted alginate droplets to the surface, the slide was left drying 10 minutes at a humidity of ~40% after spotting, Fig. 2a. Next, 0.2 M $CaCl_2$ solution was filled into each one of the 16 wells on the slide, Fig. 2b, and triggered the gelation of the droplets. The slides were stored in 0.01 M $CaCl_2$ solution to prevent dissolution of the alginate gel. Immediately before use for immunoassays,

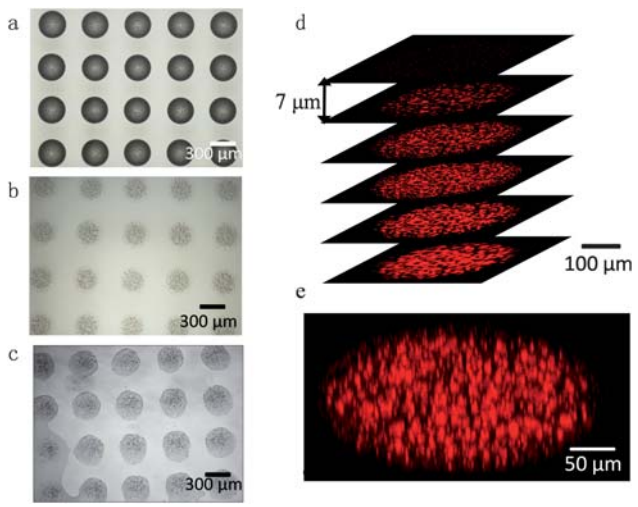

Fig. 2 Optical and confocal images of a BiGDM at different fabrication steps. (a) Optical image of the alginate solutions containing beads right after spotting. (b) Optical image of the gel-droplets immersed in $CaCl_2$ solution. (c) Optical image of the slide after removal of $CaCl_2$ solution. The spots in (c) are slightly larger and less regular shaped than those in (a) due to residual water remaining at the edge of the solidified gel-droplets and on the slide (lower left corner). (d) Confocal images taken from 0 to 35 μm every 7 μm in the *Z*-direction of a droplet immersed in $CaCl_2$ solution showing the fluorescent beads trapped inside of a gel droplet. The spot has a diameter of ~300 μm and a thickness of <35 μm as no fluorescence is visible in the last image plane. (e) Volume rendering of a beads-in-gel droplet.

the slides were incubated for 3 minutes in DI water to remove excess calcium and dried, thus, revealing the microdroplets attached to the slide, Fig. 2c. We measured the height of the droplets on a glass slide that was placed in a humidified Petri dish immediately after spotting using an upright microscope by focusing on the top surface. We measured 20 droplets and found the average height to be 40 μm, with a standard deviation of 2.4 μm. Beads-in-gel droplet structures were characterized after gelation by using microbeads coated with fluorescently labeled antibodies and a confocal microscope. An image was captured every 7 μm in the Z direction, Fig. 2d. Volume rendering of the beads-in-gel droplet structures is shown in Fig. 2e. These results indicate that the droplets were ~300 μm in diameter and <35 μm thick, and that the beads were distributed through the hydrogel. We observed that the gel droplets slightly flattened during the gelation process from ~40 μm to ~30 μm. These results indicate that the droplets adopted a disc shape, rather than a spherical shape. The disc shape is probably formed during the gelation process because following immersion of the droplet with the $CaCl_2$ solution, the surface tension responsible for the hemispheric shape disappears. Although the height of the droplets changed, it is not clear whether the change is due to geometry, or volume loss, or a combination of both. However, given that the droplets included 10% of glycerol which is hygroscopic and thus helped retain the water and mechanical integrity by preventing the droplets from drying, the volume loss is probably minor. Importantly, the beads were retained following the gelation process and the alginate adhered to the slide surface functionalized with aminosilane (see Fig. 2b).

Characterization of bead retention depending on their size

It was unclear what size of beads would be optimal and whether they could be retained within the hydrogel droplets. Therefore we evaluated different sizes of beads to identify the beads that provided the overall maximal protein binding while being retained in the hydrogel so as to maximize the assay signal. On one hand, smaller beads have a higher surface-to-volume ratio and therefore have a greater antibody binding capacity. On the other hand, the beads had to be retained in the alginate gels during the fabrication process and subsequent immunoassays. We used beads with diameters of 0.2 μm, 0.5 μm, and 1 μm functionalized with fluorescent antibodies. The fluorescence intensity of each spot before and after solidification of the gel (first and second row of Fig. 3a, respectively) was compared. A close-up of the scanned fluorescent image reveals the morphology of the gel droplets which does not exhibit the donut shape found in conventional 2D microarray spots, but appears textured instead. In alginate solutions 0.2 μm beads had the highest density of 1.67×10^{12} particles per mL and produced the highest signals likely due to the overall highest density of antibody. However, large fractions of the smaller beads with diameter 0.2 μm and 0.5 μm were washed off the gel during gelation whereas 1 μm beads were retained and gave the strongest overall signal, Fig. 3b. Based on these results, we chose 1 μm diameter beads for all immunoassays. We attributed the loss of small beads to the high porosity and mechanical softness of the alginate hydrogel. The porosity of the alginate gels prevented the usage of sub-micrometre beads, but conversely it would favor the free diffusion of proteins within the gels.

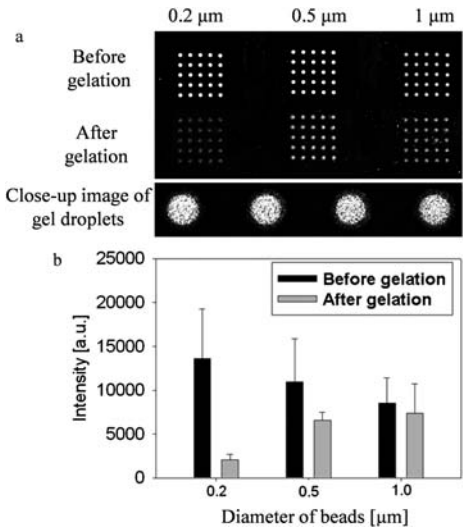

Fig. 3 Retention of beads as function of their size in the alginate gel droplets. (a) Fluorescent image of spotted beads before and after soaking in calcium solutions. Close-up of the gel droplets containing 1 μm beads. (b) Comparison of signal intensities before and after soaking. 0.2 and 0.5 μm beads revealed a significant loss of beads, whereas 1 μm beads were well retained. Error bars are the standard deviation of the 25 spots in each square.

Fluorescent signal of one-step assays as function of bead concentration and incubation time

In order to demonstrate the feasibility of BiGDM immunoassays and evaluate the effect of bead concentrations, a one-step assay was performed using different concentrations of 1 μm beads coated with Alexa 532 goat IgG to detect Alexa 647 chicken anti-goat IgG serving as an analyte. Each BiGDM was soaked for 2 h in solutions of Alexa 647 chicken anti-goat IgG antibodies with a starting concentration of 0.1 ng mL^{-1}, followed by rinsing, drying, and scanning. The fluorescent signals immobilized on the beads were used to compare signals from different concentrations of beads and to evaluate the performance of inkjet spotting. The scanned signal intensities of Alexa 532 were 31 491, 8066, and 2482 corresponding to the BiGDM beads concentrations of 3.04×10^{10} beads per mL (1×), 7.6×10^9 beads per mL (4× dilution), and 1.9×10^9 beads per mL (16× dilution). Fig. 4a shows the binding curves of the one-step assays. In these experiments, the higher the bead concentrations, the lower the detection limit and the broader the dynamic range which spanned ~5 orders of magnitude for a bead concentration of 1×; this value was used for all subsequent experiments.

In order to establish whether sample incubation time was a critical parameter, a one-step assay was performed using the 1× bead concentration. Fig. 4b shows the binding curves of the one-step assays. In the one-step format it is not possible to run a negative control without analyte, and it is thus not possible to quantify whether the difference in signal between 2 h and 1 h is due to a lower background signal or if there is an increase in sensitivity. Regardless, the difference is relatively minor, and

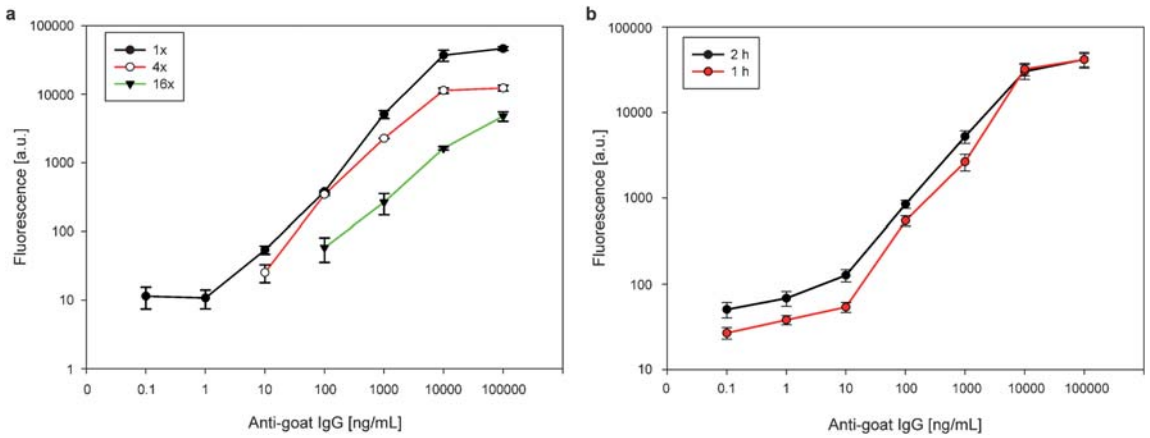

Fig. 4 (a) Binding curves of one-step assays for three different bead concentrations. Microbeads were coated with goat anti-mouse IgG to detect Alexa 647 chicken anti-goat IgG. The starting concentration was 3.04×10^{10} beads per mL and 4× and 16× dilution were tested. Fluorescent signals were obtained and the background signals were subtracted. The fluorescent signals were not detected for 4× dilution below 10 ng mL^{-1} and 16× dilution below 100 ng mL^{-1}, and hence were not shown in the figure. (b) Binding curves of one-step assays using 1 h or 2 h sample incubation time. Error bars are the standard deviation between triplicate experiments.

therefore a shorter time was selected for the final assay because it helps reduce assay time.

Multiplexed sandwich immunoassays with BiGDM platform

One of the applications of the BiGDM could be the profiling of biomarker proteins for different diseases. We selected 3 cancer related proteins, CEA, ENG, HER2, and 3 cytokines TNFα, IL-8, and CCL4/MIP-1β that have also been linked to cancer to evaluate the use of BiGDM for multiplexed sandwich immunoassays. The experimental flow is shown in Fig. 1c–f. CEA is a glycoprotein and it is the first protein biomarker for cancer demonstrated and detected in blood in 1964.[29] ENG is a cell membrane glycoprotein and functions as a part of the cell surface receptor. HER2 is a cell membrane surface receptor tyrosine kinase, and it has been used for breast cancer typing by measuring its expression in cancerous tissue by immunohistochemistry. HER2 expression is used as a criteria determining whether breast cancer patients will be treated with trastuzumab which is a monoclonal antibody against the HER2 receptor.[30] These six proteins were chosen based on results obtained in our laboratory showing that the corresponding antibody pairs displayed low cross-reactivity (Leulmi, Juncker and colleagues, unpublished work).

One of the main challenges for the previously reported hydrogel-based microarray was relatively long sample incubation time, up to 20 h due to the low permeability of the gels.[21] In our work we chose droplets because of the advantageous geometry and alginate because of the comparatively high porosity which both contribute to increase the diffusive flux to the beads and help shorten the assay time. In our assay, we used 1 h of sample incubation without agitation and obtained a high sensitivity, Fig. 5. A four-parameter logistic equation was used for fitting the binding curves.[31] 5 out of 6 curves fit the data well, showing that BiGDM produces similar binding curves than conventional immunoassays. 1 curve did not fit well the assay data suggesting that more optimization is needed. The detection limit of the assays defined as three times the standard deviation of the zero concentration signal was 18 pg mL^{-1} for CEA; 37 pg mL^{-1} for ENG; 342 pg mL^{-1} for HER2; 2.4 pg mL^{-1} for TNFα; 1 pg mL^{-1} for IL-8; and 2.3 pg mL^{-1} for CCL4/MIP-1β. However, for the curve that did not fit well (for CEA), the calculated detection limit does not reflect actual detection limits.

To explore the applicability of BiGDM in blood samples, we did a multiplexed assay for the six proteins in 10% serum, Fig. 6. The detection limit of the assays defined as three times the standard deviation of the zero concentration signal was 95 pg mL^{-1} for CEA; 114 pg mL^{-1} for ENG; 50 pg mL^{-1} for HER2; 20 pg mL^{-1} for TNFα; 5 pg mL^{-1} for IL-8; and 32 pg mL^{-1} for CCL4/MIP-1β. The detection limits in diluted serum, albeit slightly higher than in buffer, are below 100 pg mL^{-1} for 5 out of 6 proteins. The higher detection limits may be due to well known serum matrix effects,[32] or from residual concentration of the protein from the donor. For a more rigorous analysis, the concentration of proteins of interest in the samples should be verified using an independent method before spiking. The detection limits of our experiments using 10% serum are corrected by a factor 10 to take into account the dilution and compared to the physiological values found in the blood of healthy people. For CEA, ENG, and HER2 the sensitivity of BiGDM exceeds the physiological range, and for CCL4/MIP-1β, IL-8 and TNFα, it lies within it.[1,33–37] Based on the paper by Kim *et al.*,[1] the level of CEA in healthy people is 10.24 ± 5.11 ng mL^{-1} and that in breast cancer patients is 12.36 ± 8.75 ng mL^{-1}. The detection limit for CEA obtained with BiGDM is 950 pg mL^{-1}, which is ten times lower than the typical concentrations in blood. Overall, these results support the applicability of BiGDM to multiplexed protein profiling of blood.

To the best of our knowledge this represents the first example of a BiGDM and it paves the way for multiplexed protein profiling on a larger scale. Upon optimization of the beads concentration and evaluation of sample incubation time, the binding curves for these assays reached down to low pg mL^{-1} range for 1 h of sample incubation. Further reducing the sample incubation time may lead to reduced limits of detection, and should be evaluated for each antibody pair used for BiGDM. To

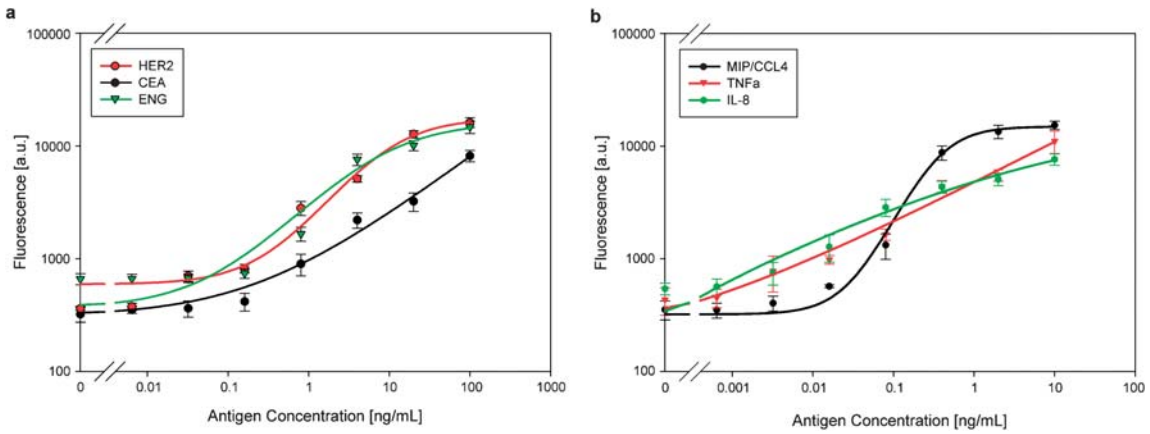

Fig. 5 Binding curves for sandwich immunoassays for six proteins in buffer solutions. Curve fitting was performed based on four-parameter logistic equation by SigmaPlot software. (a) Assay results and binding curves for CEA, ENG, and HER2 for concentration from 100 ng mL^{-1} down to 0.01 ng mL^{-1}. (b) Assay results and binding curves for TNFα, IL-8, and CCL4/MIP-1β from 10 ng mL^{-1} down to 0.001 ng mL^{-1}; the affinity of the antibodies for these three proteins was higher and the assay range was adjusted accordingly. The spots on the left are the negative control signals with zero antigen concentration. The error bars are standard deviations between triplicate experiments.

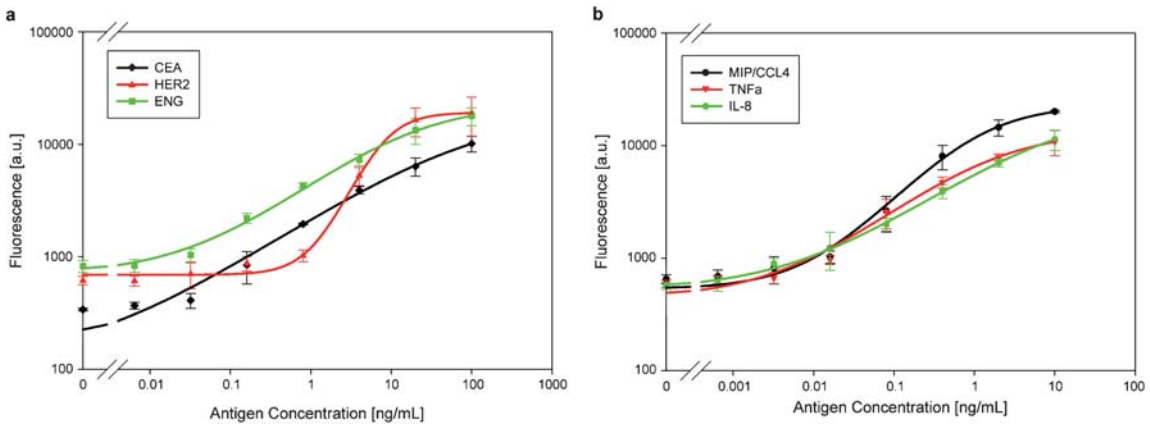

Fig. 6 Binding curves for sandwich immunoassays for six proteins in a 10% serum solution. Curve fitting was performed based on four-parameter logistic equation by SigmaPlot software. (a) Assay results and binding curves for CEA, ENG, and HER2 for concentration from 100 ng mL^{-1} down to 0.01 ng mL^{-1}. (b) Assay results and binding curves for TNFα, IL-8, and CCL4/MIP-1β from 10 ng mL^{-1} down to 0.001 ng mL^{-1}. The spots on the left are the negative control signals with zero antigen concentration. The error bars are standard deviations between triplicate experiments.

further improve assay sensitivity, we agitated sample solutions with a microarray shaker. However, after shaking at 100 rpm for 1 h, the top of the droplets was removed and a rough surface formed. We suspect that due to the softness of alginate hydrogels, the mechanical stress during the shaking process was sufficient to damage the droplets.

Conclusions

In this work we developed a novel 3D BiGDM for multiplexed sandwich immunoassays in an array format by using one micrometre antibody coated microbeads trapped in space within hydrogel droplets. This configuration spreads capture antibodies in 3D space and makes them more accessible to their antigens relative to 2D surfaces thus reducing mass transport limitations. Previous work on 3D hydrogel microarrays achieved ng mL^{-1} detection limits for prostate-specific antigen (PSA) with 17 h incubation on glass substrate and 2 h incubation on metal-coated substrate which enhanced fluorescent signals.[20,21] The detection limit of BiGDM with 1 h sample incubation varied between 5 pg mL^{-1} and 114 pg mL^{-1} for IL-8 and ENG, respectively, which constitutes a major improvement which we ascribe to the porosity of alginate gels. In addition, the fabrication procedure for BiGDM is simple and inexpensive, and can be used for other alginate-based microarray applications.

We thus believe that BiGDM have a potential for multiplexed profiling of proteins for analytical applications. Finally, if a hydrogel could be found that is both highly porous and mechanically robust, it might be possible to further enhance the mass transport and reduce the assay time by using agitation for mixing, or by using microfluidics for encapsulating the hydrogel droplets within a channel for flushing the reagents.[24]

Acknowledgements

We thank the Canadian Institutes for Health Research (CIHR), Genome Canada, Genome Quebec, the Natural Science and Engineering Research Council of Canada (NSERC) and the

Canada Foundation for Innovation (CFI) for financial support. D.J. acknowledges support from a Canada Research Chair.

References

1 B. K. Kim, J. W. Lee, P. J. Park, Y. S. Shin, W. Y. Lee, K. A. Lee, S. Ye, H. Hyun, K. N. Kang, D. Yeo, Y. Kim, S. Y. Ohn, D. Y. Noh and C. W. Kim, *Breast Cancer Res.*, 2009, **11**, DOI: 10.1186/bcr2247.
2 M. Arellano-Garcia, S. Hu, J. Wang, B. Henson, H. Zhou, D. Chia and D. T. Wang, *Oral Dis.*, 2008, **14**, 705–712.
3 S. S. Khan, M. S. Smith, D. Reda, A. F. Suffredini and J. P. McCoy, *Cytometry B Clin. Cytom.*, 2004, **61**, 35–39.
4 P. Angenendt, J. Glokler, Z. Konthur, H. Lehrach and D. J. Cahill, *Anal. Chem.*, 2003, **75**, 4368–4372.
5 W.-M. Gao, R. Kuick, R. P. Orchekowski, D. E. Misek, J. Qiu, A. K. Greenberg, W. N. Rom, D. E. Brenner, G. S. Omenn, B. B. Haab and S. M. Hanash, *BMC Cancer*, 2005, **5**, 110.
6 A. Carlsson, C. Wingren, J. Ingvarsson, P. Ellmark, B. Baldertorp, M. Ferno, H. Olsson and C. A. K. Borrebaeck, *Eur. J. Cancer*, 2008, **44**, 472–480.
7 R. Rimini, J. M. Schwenk, M. Sundberg, R. Sjoberg, D. Klevebring, M. Gry, M. Uhlen and P. Nilsson, *J. Proteomics*, 2009, **73**, 252–266.
8 W. Kusnezow, A. Jacob, A. Walijew, F. Diehl and J. D. Hoheisel, *Proteomics*, 2003, **3**, 254–264.
9 E. W. Olle, J. Messamore, M. P. Deogracias, S. D. McClintock, T. D. Anderson and K. J. Johnson, *Exp. Mol. Pathol.*, 2005, **79**, 206–209.
10 C. Wingren, J. Ingvarsson, L. Dexlin, D. Szul and C. A. K. Borrebaeck, *Proteomics*, 2007, **7**, 3055–3065.
11 E. Delamarche, D. Juncker and H. Schmid, *Adv. Mater.*, 2005, **17**, 2911–2933.
12 M. Pla-Roca, R. F. Leulmi, H. Djambazian, S. Sundararajan and D. Juncker, *Anal. Chem.*, 2010, **82**, 3848–3855.
13 D. M. Marsden, R. L. Nicholson, M. Ladlowb and D. R. Spring, *Chem. Commun.*, 2009, 7107–7109.
14 C. Preininger, U. Sauer, S. Obersriebnig and M. Trombitas, *Int. J. Environ. Anal. Chem.*, 2005, **85**, 645–654.
15 K. Derwinska, U. Sauer and C. Preininger, *Talanta*, 2008, **77**, 652–658.
16 K. Derwinska, L. A. Gheber and C. Preininger, *Anal. Chim. Acta*, 2007, **592**, 132–138.
17 Y. Zhou, O. Andersson, P. Lindberg and B. Liedberg, *Microchim. Acta*, 2004, **147**, 21–30.
18 P. T. Charles, E. R. Goldman, J. G. Rangasammy, C. L. Schauer, M.-S. Chen and C. R. Taitt, *Biosens. Bioelectron.*, 2004, **20**, 753–764.
19 L.-L. Lv, B.-C. Liu, C.-X. Zhang, Z.-M. Tang, L. Zhang and Z.-H. Lu, *Electrophoresis*, 2007, **28**, 406–413.
20 D. A. Zubtsov, E. N. Savvateeva, A. Y. Rubina, S. V. Pan'kov, E. V. Konovalova, O. V. Moiseeva, V. R. Chechetkin and A. S. Zasedatelev, *Anal. Biochem.*, 2007, **368**, 205–213.
21 Z. I. Zubtsova, D. A. Zubtsov, E. N. Savvateeva, A. A. Stomakhin, V. R. Chechetkin, A. S. Zasedatelev and A. Y. Rubina, *J. Biotechnol.*, 2009, **144**, 151–159.
22 A. Y. Rubina, A. Kolchinsky, A. A. Makarov and A. S. Zasedatelev, *Proteomics*, 2008, **8**, 817–831.
23 P. W. Stevens, C. H. J. Wang and D. M. Kelso, *Anal. Chem.*, 2003, **75**, 1141–1146.
24 M. Ikami, A. Kawakami, M. Kakuta, Y. Okamoto, N. Kaji, M. Tokeshi and Y. Baba, *Lab Chip*, 2010, DOI: 10.1039/C0LC00241K.
25 M. Bally, J. Voros and S. Takeuchi, *Lab Chip*, 2010, **10**, 372–378.
26 D. O. Fesenko, T. V. Nasedkina, A. V. Chudinov, D. V. Prokopenko, R. A. Yurasov and A. S. Zasedatelev, *Mol. Biol.*, 2005, **39**, 96–102.
27 M.-Y. Lee, C. B. Park, J. S. Dordick and D. S. Clark, *Proc. Natl. Acad. Sci. U. S. A.*, 2005, **102**, 983–987.
28 M.-Y. Lee, R. A. Kumar, S. M. Sukumaran, M. G. Hogg, D. S. Clark and J. S. Dordick, *Proc. Natl. Acad. Sci. U. S. A.*, 2008, **105**, 59–63.
29 P. Gold and S. O. Freedman, *J. Exp. Med.*, 1965, **121**, 439–462.
30 J. M. Harvey, G. M. Clark, C. K. Osborne and D. C. Allred, *J. Clin. Oncol.*, 1999, **17**, 1474–1481.
31 J. W. A. Findlay and R. F. Dillard, *AAPS J.*, 2007, **9**, E260–E267.
32 C. Pfleger, N. Schloot and F. t. Veld, *J. Immunol. Methods*, 2008, **329**, 214–218.
33 Z. A. Dehqanzada, C. E. Storrer, M. T. Hueman, R. J. Foley, K. A. Harris, Y. H. Jama, C. D. Shriver, S. Ponniah and G. E. Peoples, *Oncol. Rep.*, 2007, **17**, 687–694.
34 N. Takahashi, R. Kawanishi-Tabata, A. Haba, M. Tabata, Y. Haruta, H. Tsai and B. K. Seon, *Clin. Cancer Res.*, 2001, **7**, 524–532.
35 Z. R. Yurkovetsky, J. M. Kirkwood, H. D. Edington, A. M. Marrangoni, L. Velikokhatnaya, M. T. Winans, E. Gorelik and A. E. Lokshin, *Clin. Cancer Res.*, 2007, **13**, 2422–2428.
36 S.-Y. Kong, J. H. Kang, Y. Kwon, H.-S. Kang, K.-W. Chung, S. H. Kang, D. H. Lee, J. Ro and E. S. Lee, *J. Clin. Pathol.*, 2006, **59**, 373–376.
37 U. Berberoglu, E. Yildirim and O. Celen, *Int. J. Biol. Markers*, 2004, **19**, 130–134.